

Pinning retrofit technique in masonry with application of polymer-cement pastes as bonding agents

Kshitij C. Shrestha^{1a}, Sanjay Pareek^{2b}, Yusuke Suzuki^{3c} and Yoshikazu Araki^{*1}

¹Department of Architecture and Architectural Engineering, Graduate School of Engineering,
Kyoto University, Kyoto 615-8540, Japan

²Department of Architecture, College of Engineering, Nihon University, Koriyama,
Fukushima 963-8642, Japan

³International Research Institute of Disaster Science, Tohoku University, Aoba Sendai 980-8579, Japan

(Received April 18, 2013, Revised June 20, 2013, Accepted July 6, 2013)

Abstract. This paper reports extensive experimental study done to compare workability and bond strength of five different types of polymer-based bonding agents for reinforcing bars in pinning retrofit. In pinning retrofit, steel pins of 6 to 10 mm diameters are inserted into holes drilled diagonally from mortar joints. This technique is superior to other techniques especially in retrofitting historic masonry constructions because it does not change the appearance of constructions. With an ordinary cement paste as bonding agent, it is very difficult to insert reinforcing bars at larger open times due to poor workability and very thin clearance available. Here, open time represents the time interval between the injection of bonding agent and the insertion of reinforcing bars. Use of polymer-cement paste (PCP), as bonding agent, is proposed in this study, with investigation on workability and bond strengths of various PCPs in brick masonry, at open times up to 10 minutes, which is unavoidable in practice. Corresponding nonlinear finite element models are developed to simulate the experimental observations. From the experimental and analytical study, the Styrene-Butadiene Rubber polymer-cement paste (SBR-PCP) with prior pretreatments of drilled holes showed strong bond with minimum strength variation at larger open times.

Keywords: masonry retrofitting; pinning retrofit technique; polymer-cement paste; pretreatments; barrier impregnants; bonding agent; finite element modeling

1. Introduction

Recognizing the shortcoming of unreinforced masonry (URM) walls, there has been a surge of interest in recent years to develop techniques for improving their seismic behavior. Among various available retrofitting techniques (Abrams *et al.* 2007, Calderini 2008, Curti *et al.* 2008, Willis *et al.* 2010, Ashraf *et al.* 2012), there exist ample difficulties associated with the preservation of historical masonry constructions, durability of strengthening materials, and also restriction on the parts of a construction to be retained. Pinning retrofit procedure, practiced in Japan, has strong

* Corresponding author, Associate Professor, E-mail: araki@archi.kyoto-u.ac.jp

^a Ph.D., E-mail: se.kshitij@archi.kyoto-u.ac.jp

^b Ph.D., E-mail: pareek@arch.ce.nihon-u.ac.jp

^c Ph.D., E-mail: ysuzuki@irides.tohoku.ac.jp

potential in masonry retrofitting since in addition to strength and ductility improvements, this technique also causes minimal change in original appearance of structures. Here, retrofitting is done by inserting inclined stainless steel bars in to the walls as shown in Fig. 1. This technique has the advantages of facilitating construction with no need to remove roof and change the foundation during retrofitting process, lowering the construction cost and shortening the construction period. Extensive experimental (Takiyama *et al.* 2008) and numerical (Shrestha *et al.* 2011a,b) studies were done to demonstrate the robustness of this pinning retrofit technique in masonry constructions. To the authors' knowledge, pinning retrofit procedure involves the use of epoxy resin for bonding between masonry and reinforcing bar, which even though provides a good workability environment during construction process, but epoxy resin, being an organic adhesive, has limitations, such as low fire resistance, higher cost, high stiffness and poor bond to wet surfaces.

During pinning retrofit, a professional mason would require an open time limit up to 10 minutes between injection of mortar paste and insertion of reinforcing bar. Here, open time represents the time interval between the injection of bonding agent and the insertion of reinforcing bars as shown schematically in Fig. 2. With an ordinary mortar paste as bonding agent, however, it is very difficult to insert reinforcing bars at larger open times due to its poor workability and small clearance available. Moreover, brick units absorb water from mortar pastes in absence of any water barrier penetrants. As an alternative, use of polymer-cement paste (PCP) as bonding agent is proposed in this study with investigation on workability and bond strengths of various polymer based admixtures in brick masonry. Fig. 3 illustrates the above described scenario and main purpose of this proposed research.

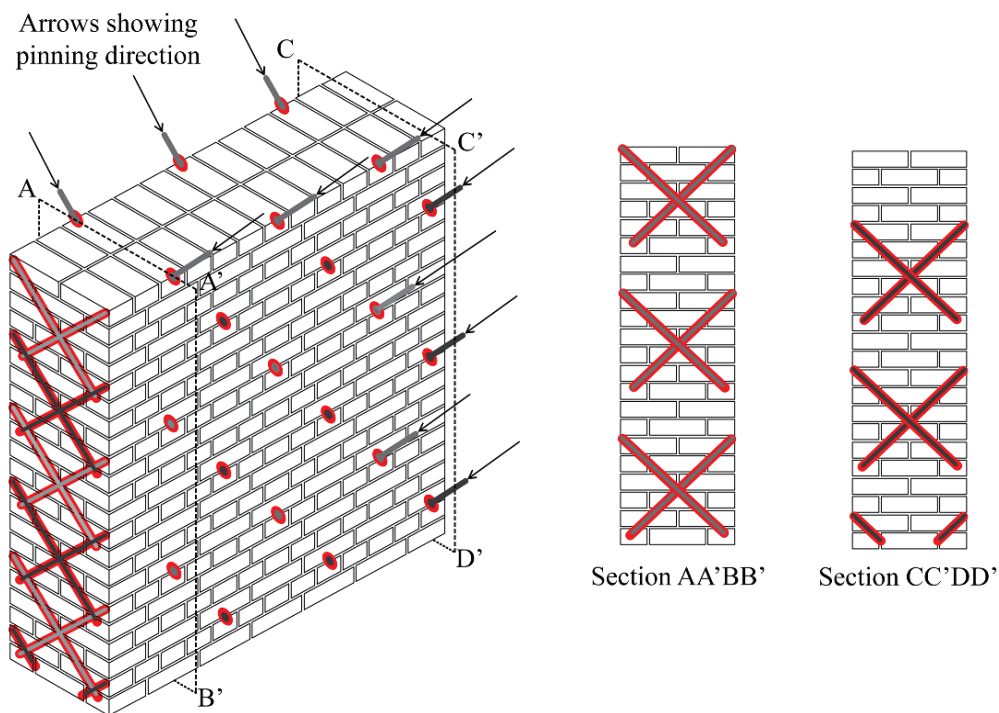


Fig. 1 Cross pinning retrofit technique

Mechanical properties of polymer-based cementitious bonding agents as PCP and polymer-cement mortar (PCM) have already been reported as highly superior over normal conventional mortar (Pareek and Kuroda 2003, Ohama 1995, 1998, Fowler 1999, Maranhao and John 2009). Latex-modified mortar provides an improved workability over normal cement mortar and also with increase in polymer-cement ratio, there is a subsequent reduction in water-cement ratio, which ultimately contributes to strength development and drying shrinkage reduction. In hardened state, PCM shows an improved water-proofness and improved bond strength over ordinary cement mortar which makes PCP and PCM a potential bonding material in retrofitting URM.

Application of PCP to masonry retrofit requires another important consideration regarding workability. If applied to masonry in its normal state, water in PCP gets absorbed by masonry making the PCP's workability poor. For this reason, pretreatment of masonry is necessary to create a water penetration barrier film so that there is minimum effect on workability of PCP after insertion. The present study involves comparison on various pretreatment agents and their effect on workability of PCP in masonry.

The use of PCM for repair and restoration purpose of masonry structures has been limited to its use more as surface coating over grid of reinforcing bars (Kikuchi *et al.* 2008, Anagnostopoulos and Anagnostopoulos 2002, Faella *et al.* 2010) on unreinforced masonry walls. In this study, we examine and compare the effectiveness of PCPs prepared from various polymer admixtures, as bonding adhesive between reinforcing bar and masonry, considering the effect of pretreatment.

2. Test program

2.1 Materials

2.1.1 Brick unit

Normal Japanese brick units of sizes 210×100×60 mm prescribed by JIS R 1250 were used. Water absorption tests done on 3 brick units of sizes 210×100×60 mm showed an average absorption rate of 6.73% with standard deviation of 0.47%. Additionally, 6 samples of brick units tested showed an average compressive strength of 51.46 MPa with standard deviation of 2.43 MPa observed during the tests.

2.1.2 Mortar

Mortar joint for masonry assemblage was prepared with ordinary Portland-cement, sand and water at 1:3:0.5 ratios. Total six cylindrical test pieces of the mortar with diameter 50 mm and height 100 mm were prepared for compressive strength (3nos.) and split tensile strength (3nos.) determination. The average value of compressive strength was 36.57 MPa with standard deviation of 2.7 MPa. Additionally, split tensile tests showed an average split tensile strength value of 4.24 MPa at standard deviation of 0.24 MPa.

Tensile adhesion tests were also done on total 10 samples of brick-mortar joints to check interface bond strength between brick unit and mortar joint. An average tensile adhesive strength of 1.03 MPa at standard deviation of 0.83 MPa was obtained.

The adhesive tensile strength of mortar used in the test specimens is comparatively higher. The choice of such relatively high mortar tensile strength was made by considering the restrictions on the loading machine and the loading arrangement.

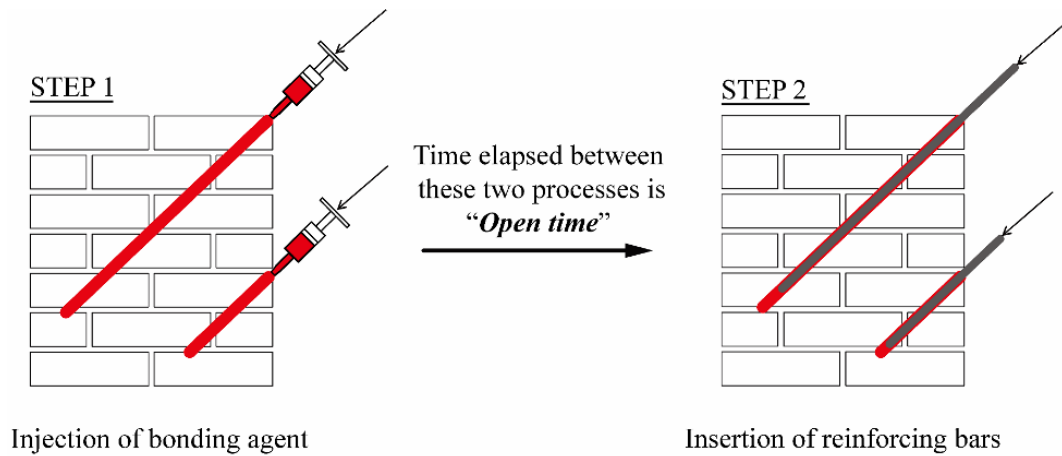


Fig. 2 Open time during pinning technique

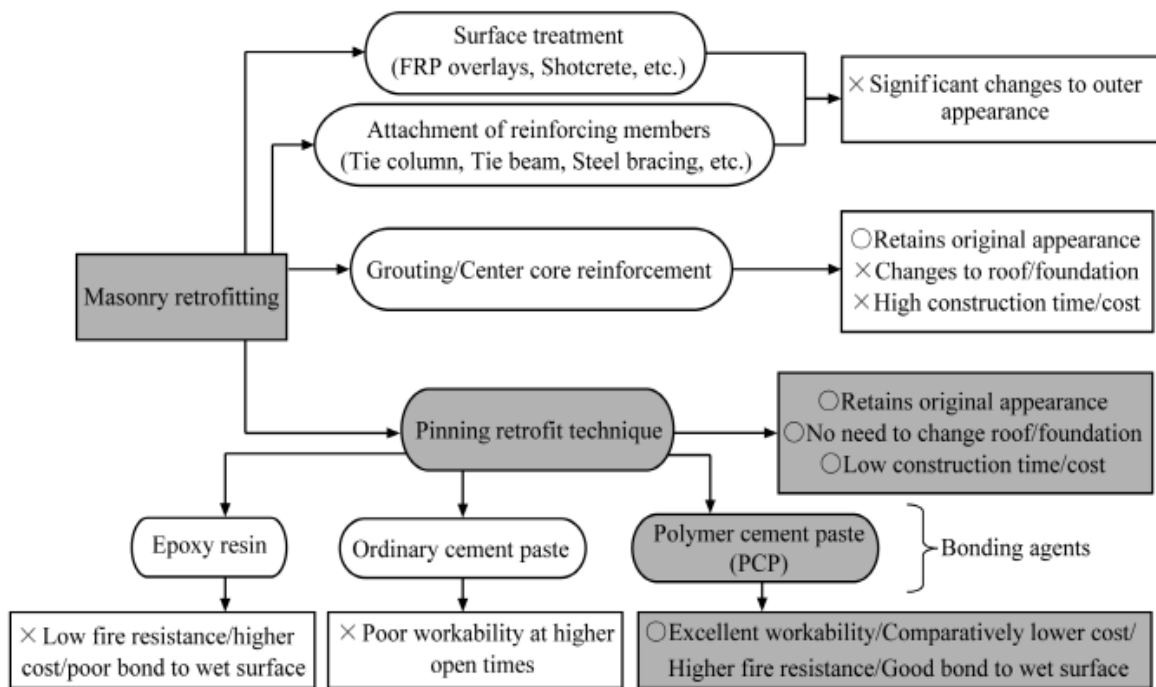


Fig. 3 Comparison on different masonry retrofitting techniques and purpose of the present work

In this study, 3-point bending tests were performed with specimens placed horizontally on the supports as illustrated later in Section 2.2.2. Such loading arrangement would have possibly resulted in cracking of URM specimen during the test specimen placing due to its self-weight. In order to avoid such scenario, the comparatively higher adhesive tensile strength was adopted. However, more importantly, the use of this mortar class essentially does not affect the post-cracking behavior of the masonry beam specimens during bending tests. Here, after the

initiation of mortar joint cracking, the response is primarily governed by bond slip along the re-bars and masonry. It should be noted that better interpretation of actual on-site condition may be made through the use of lower strength mortar.

2.1.3 Reinforcing bars

Fully threaded steel bars of diameter 6 mm were used as reinforcing bars for retrofitting purpose. Tensile tests performed on three bar samples showed an average fracture stress of 654 MPa and average fracture strain of 2.36%.

2.1.4 Polymer based admixtures

Five different types of polymer admixtures used in this study were -- EVA, ACL, PAE, SBR1 and SBR2, representing one of the most popular commercially used polymers (Ohama 1995). The corresponding nomenclature and properties of the above mentioned polymer dispersions are given in Table 1. The corresponding PCPs for the above listed polymers were prepared using ordinary Portland-cement with polymer-cement ratio (P/C) of 20% and water-cement ratio (W/C) at 40%.

2.1.5 Water penetration barrier agents (Impregnants)

Three types of alkyl alkoxysilane based barrier penetrants (BPs) or impregnants were used – BPA-I, BPA-II and BPC-I in this study. These three BPs were chosen after proper water absorption rate tests were done on brick unit specimen with seven different commercially available BPs. Additionally, application of water and polymers as water penetration barrier agents in place of impregnants was also examined.

2.2 Specimens and test descriptions

2.2.1 Workability and pull-out test

The first phase of the experiment involved workability tests for different PCPs with pre-application of the above mentioned impregnants. Ordinary Portland-cement with polymer-cement ratio (P/C) of 20% and water-cement ratio (W/C) at 40% was adopted for all the mixes. These proportions were determined after extensive sensitivity and trial and error studies on PCPs used. Each specimen, as shown in Fig. 4, first involved drilling of 8 mm diameter holes 100 mm deep on 100×105×60 mm³ well-cut brick samples. Dusts in the holes were blown out by applying air pressure. Afterwards 25 cm³ of impregnant was injected into the hole as shown in Fig. 5. After 60 minutes of impregnant injection, PCP was injected into the hole. A 6 mm diameter fully threaded steel bar was inserted into the hole at three different open times -- 0 minute, 5 minutes and 10 minutes for each type of impregnant and PCP. The specimen was placed over digital weighing balance and the amount of force required for the insertion of pin was recorded to measure the workability as shown in Fig. 6.

Additional tests were also performed using polymer and water in place of impregnants for the pretreatment. In case of polymer, polymer used in corresponding PCP was used in two different ways. For Polymer-I, polymer was injected into the hole and was poured out within 30 minutes followed by PCP injection. However, in case of Polymer-II, PCP was injected into the holes after drying polymer for 5 days after pretreatment of the hole. For comparison, untreated specimens without application of any water penetration barrier agents, termed as untreated specimen here onwards, were also prepared. 3 samples of specimens were prepared for each test ID. For each PCP type, (7 pretreatments x 3 open times x 3 samples) 63 specimens were prepared with different

Table 1 Properties of polymer dispersion

Type of polymer	Chemical constituent	Viscosity (mPa.s)	Mechanical properties of polymer-cement paste		
			E (GPa)	f_c (MPa)	ν
EVA	Ethylene vinyl acetate copolymer emulsion	1000±200	18.2	43.19	0.24
ACL	Acrylic polymer dispersion	14	15.5	44.21	0.20
PAE	Polyacrylic ester emulsion	300	12.9	35.29	0.21
SBR1	Styrene-butadiene rubber latex	200	17.6	49.78	0.22
SBR2	Styrene-butadiene rubber latex	50	19.7	50.10	0.20

E - Young's modulus, f_c - Compressive strength, ν - Poisson's ratio

pretreatments and tested at different open times. To summarize, a total of 315 specimens were prepared for all PCPs to test the workability. Direct pull-out tests of steel bars were performed on each of above prepared specimens to compare the bond strength of the PCP in brick masonry as shown in Fig. 7(a). Curing for test specimen was performed for 28 days at 90% relative humidity prior to pull-out tests. The above sequence of workability and pull-out test plan is illustrated in Fig. 7(b).

2.2.2 Out-of-plane bending test

Fig. 8 shows the test set-up for masonry beam specimen with dimensions 1040×320×320 mm. Fig. 9 illustrates the procedures involved in the reinforced masonry beam specimen preparation. Two sets of each PCP bonded specimens were prepared. Three types of different polymer admixtures were used in this study – SBR2, ACL and PAE. These three PCPs were chosen based on previously performed workability and bond strength tests, where SBR2 and PAE were found among the high ranked bonding agent (with better workability and bond strength) and ACL the least ranked one.

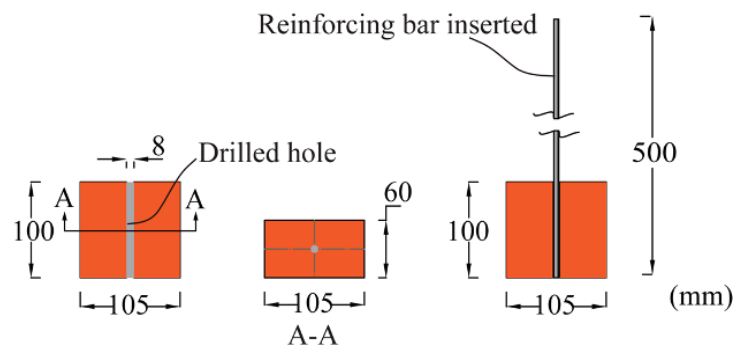


Fig. 4 Details of test specimen for workability and pull-out tests



Fig. 5 Impregnant injection in drilled holes



Fig. 6 Workability test procedure

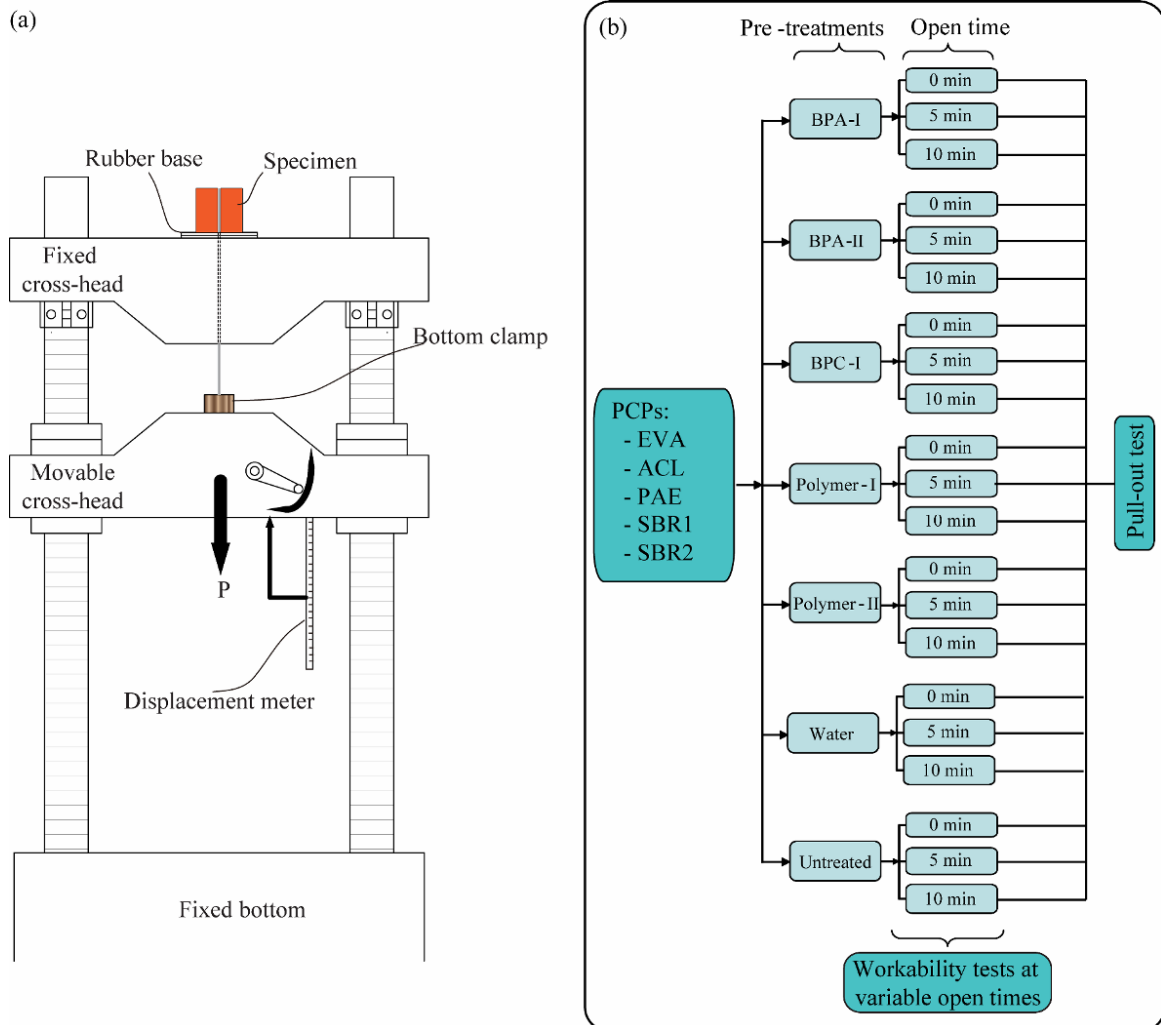


Fig. 7 Test program: (a) Pull-out test set-up, (b) Workability and pull-out test plan

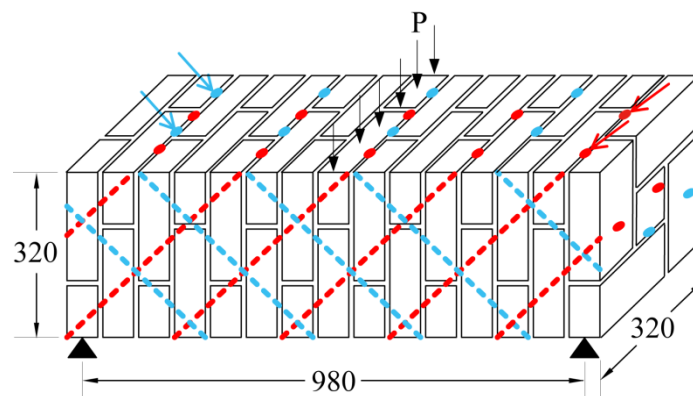
Such adverse conditions allow better comparison on the effect of bond strength on out-of-plane response of masonry and effective interpretation of test results. PCPs for the above listed polymers were prepared using ordinary Portland-cement with polymer-cement ratio (P/C) of 20% and water-cement ratio (W/C) at 40% for all the mixes. One set of URM and epoxy resin bonded (ER) specimens were also prepared for comparison with PCP bonded specimens. For the reinforced specimens, fully threaded 6mm diameter reinforcing bars were used. Points of insertion of reinforcing bars on masonry beam specimen are shown in Fig. 8 with all bars inserted from the top face as illustrated in Figs. 8 and 9. The present study involves use of BPA-II as impregnant for all the PCP bonded specimens. The choice of BPA-II as impregnant was decided on the basis of workability tests and bond strength tests performed previously with different types of impregnants available.

For reasonable assessment of the seismic performance of masonry structures, effectiveness of the proposed retrofitting technique to the in-plane shear load is also required. Furthermore, the impact of in-plane shear load on the out-of-plane collapse in the global building response needs to be verified with proper experimentations. The present experimental work with the use of PCP is limited to the out-of-plane response of masonry wall. Nevertheless, good estimation and simulation to represent in-plane shear behavior of the proposed retrofitting technique can be studied by developing finite element and analytical models (Shrestha *et al.* 2011b).

3. Experimental results

3.1 Workability test

The test arrangement is shown in Fig. 6 where the polymer injected brick is placed over the digital weighing balance. Workability is measured by the record of insertion load required for vertical insertion of a reinforcing bar into the hole at variable open times. Figs. 10(a) and (g) show the results for the workability tests of PCPs with different pretreatments performed. Here, better workability is reflected by lower values for insertion load which represents easier insertion of reinforcing bars. Plots are made with average value of insertion load of the 3 identical samples



All dimensions in mm

Fig. 8 Specimen and test set-up for three-point bending test

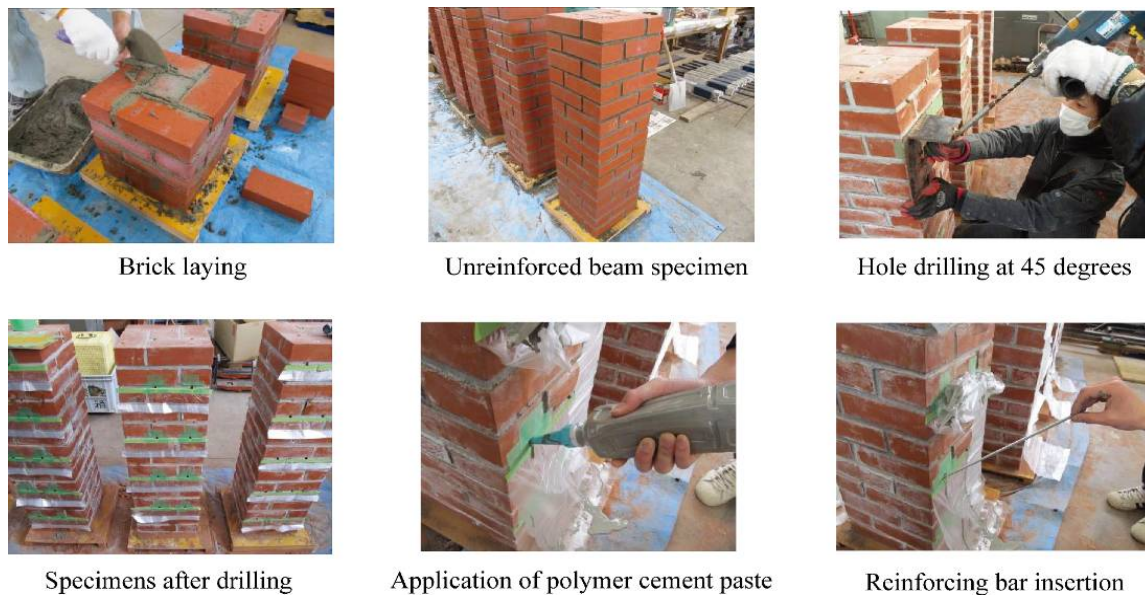


Fig. 9 Preparation of beam specimen for pinning retrofit

tested. The corresponding error bars shown in Fig. 10 represents the standard deviation of experimentally recorded data at particular open time for identical specimens. At open time of 0 minute, all combination of pretreatments with PCPs showed good workable response as shown in Fig. 10. In most cases, increase of open time led to increase of the load necessary for inserting reinforcing bars. The rates of increase however were significantly different depending on the type of PCPs used. With increment in open time up to 5 minutes with results given in Fig. 10(e), reinforcing bars could not be inserted in case of ACL PCP when pretreated with Polymer-II. For open time of 10 minutes, following combinations of pretreatment and PCPs were not workable: i) Polymer-I pretreated ACL PCP in Fig. 10(d), ii) Polymer-II pretreated ACL, SBR2 and SBR1 PCPs in Fig. 10(e), iii) water pretreated ACL PCP in Fig. 10(f), and iv) Untreated ACL, EVA and PAE PCPs in Fig. 10(g). For impregnants, BPA-I, BPA-II and BPC-I, pretreated specimens, all PCPs used were workable for open times up to 10 minutes.

Workability tests showed that pretreatment plays an important role in keeping the PCP workable for longer duration of time. Use of impregnants -- BPA-I, BPA-II and BPC-I, as well as water all significantly increased the workability of all the PCPs used. Tests, on the use of polymer itself as a water penetration barrier system, did not show positive results. In fact, Polymer-II adversely affected the workability of the PCPs due to the formation of a thick layer of polymer film by drying, with its response inferior even compared to the untreated specimens. Untreated specimens also showed relatively inferior workability environment.

3.2 Pull-out test

Direct pull-out test results on steel bars of the specimens are shown in Figs. 11 and 12. Fig. 11 shows the failure patterns observed for pull-out test results. Three different types of failure patterns were observed during the pull-out tests: (a) bond slip along PCP joint interface, (b) tensile failure of reinforcing bar, and (c) brick failure as shown in Fig. 11. For impregnant pretreated specimens,

majority of tests, around 75%, showed pull out with failure of bond slip as illustrated in Fig. 11(a). For EVA, ACL, PAE PCPs, pull-out tests showed bond slip along PCP joint for all the impregnated pretreated specimens. However, for SBR1 and SBR2 PCPs injected specimens, pretreated with impregnants or water, slightly higher bond strengths were observed, with some of the tests resulting in tensile fracture of reinforcing bars as shown in Fig. 11(b). This showed the superiority of SBR1 and SBR2 over other PCPs. 23.75% of pull-out tests resulted in fracture of reinforcing bar and 1.25% in brick failure.

Plots, in Figs. 12 (a) and (g), are made for the average value of pull out load recorded for 3 identical samples of specimens and the variations in the results are shown by the error bars, representing the standard deviation of sample data. A dotted line, representing the limit for fracture of reinforcing bar, is also shown, assume the tensile strength of steel bars used to be 650 MPa and effective diameter of steel bars 5.5 mm. Pull-out test results are shown for specimens with three impregnants -- BPA-I, BPA-II and BPC-I, polymer treated, water treated and untreated. ACL and PAE PCPs showed the least of bond strength among the used PCPs. EVA, SBR1 and SBR2 showed comparatively better bond strengths. Also bond strength of each PCP was largely affected by other two factors -- open time and pretreatment agent. With an increase in open time, average bond strength of PCP decreased in most of the cases.

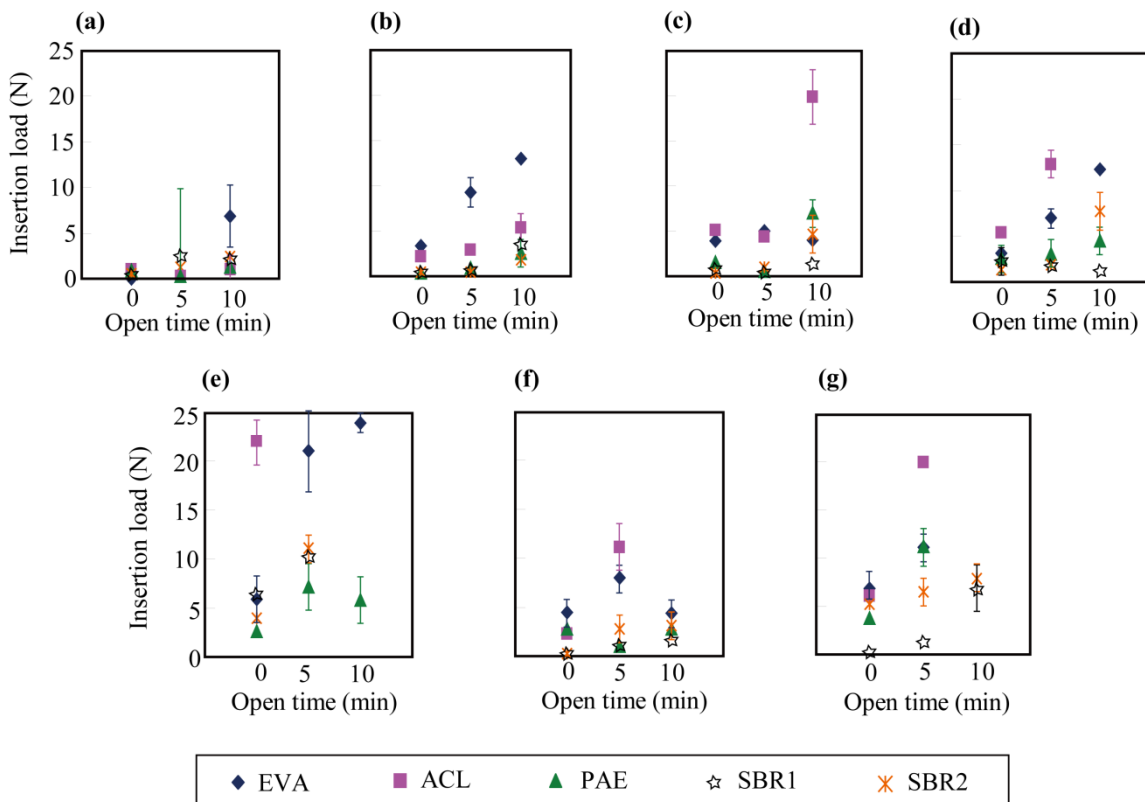


Fig. 10 Insertion load for combination of PCPs and impregnants at varying open times: (a) BPA-I, (b) BPA-II, (c) BPC-I, (d) Polymer-I, (e) Polymer-II, (f) Water treated, (g) Untreated

Better PCP would be the one which shows better bond strength even at longer open time, or the one which shows lesser variation of bond strength at variable open time sets. More detailed discussions on this aspect are presented later in Section 5. SBR PCPs injected specimens with pretreatments involving either impregnants or water showed superior bond strength as compared to other combinations.

3.3 Bending test

3.3.1 Test observations

Fig. 13 shows the resisting force versus rotation angle plot for all the specimens. Fig. 13(a) shows the response up to rotation angle of 0.01 radian and Fig. 13(b) illustrates the response for larger deformation range up to 0.02 radian. Here, rotation angle of the tested specimen represents the deformation experienced by the specimen as illustrated in Fig. 13. For the URM specimen, after the initiation of the first crack at around 15 kN of resisting force and very small deformation angle, the specimen cracked with no resistance shown afterwards. For ER-RM specimen, the maximum resisting force of around 32 kN was observed larger than for any of other specimens. This large resisting force was contributed by strength of epoxy resin itself, whose bond strength is relatively higher. However, for ER-RM specimen, large stress concentration possibly resulted in brittle fracture of the steel bar at relatively smaller rotation angle of 0.018 radian as shown in Fig. 13(b). Among the PCP bonded specimens, SBR-RM specimens showed comparatively better response, with no fracture of reinforcing bars. ACL-RM and PAE-RM specimens on the other hand showed relatively lower value of resisting force. The responses observed above in Fig. 13 have also been compared with theoretical computations as described below.

3.3.2 Fracture mechanisms and theoretical predictions

Cracks observed for the specimens were as shown in Figs. 14-15, varied in accordance with the reinforcing type of the specimens. ER-RM, SBR-RM1 and SBR-RM2 specimens showed “Mode-1” failure shown in Figs. 14 and 15 (left). For URM and ACL-RM1 specimens, “Mode-2” failure as shown in Fig. 15 (center) was observed.

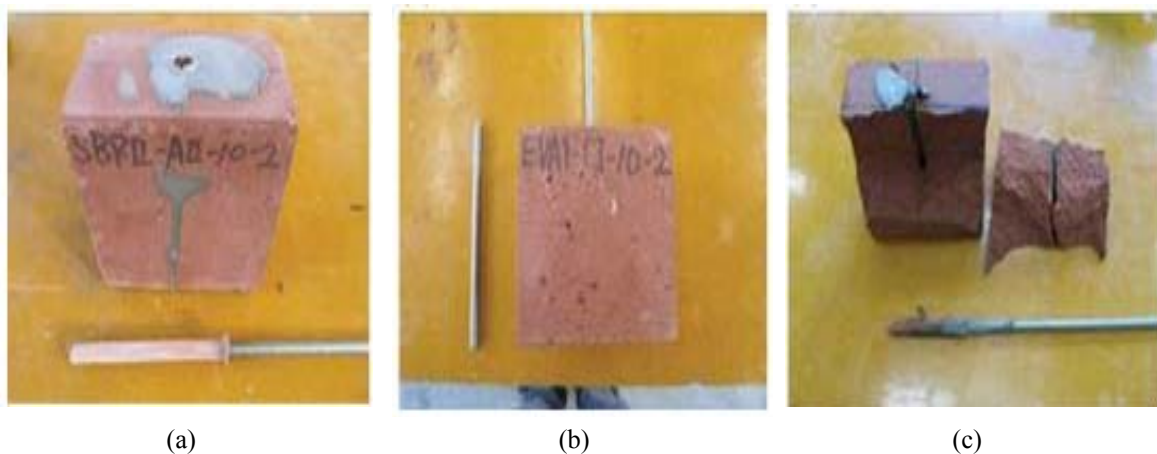


Fig. 11 Failure patterns observed during pull-out tests: (a) Bond slip along PCP, (b) Tensile failure of reinforcing bar and (c) Brick failure

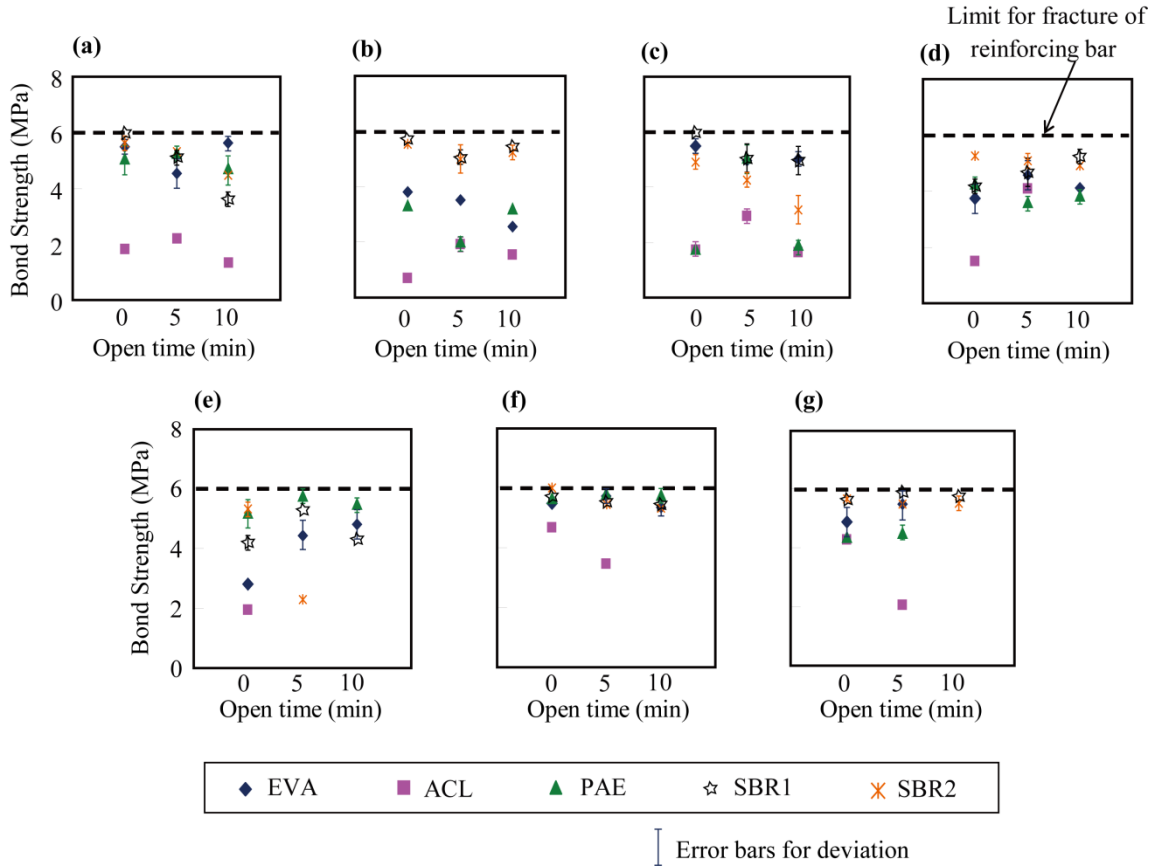


Fig. 12 Average bond strength from pull-out tests on specimens prepared at varying open times: (a) BPA-I, (b) BPA-II, (c) BPC-I, (d) Polymer-I, (e) Polymer-II, (f) Water treated and (g) Untreated

ACL-RM2, PAE-RM1 and PAE-RM2 specimens showed cracks at different place, at second mortar joint to right from the center shown as “Mode-3” failure in Fig. 15 (right). The prediction of crack in masonry is very difficult, mainly attributed by the fact that there exists large deviation in bond strength of mortar joints from specimen to specimen.

Reinforcing bar fracture mechanism

For ER-RM specimen, where failure mechanism was actuated by fracture of reinforcing bar, resisting force was predicted assuming a free-body as shown in Fig. 14(b), neglecting the bed-joint tensile strength. Equilibrium condition for the given free bodies can be expressed as follows

$$\begin{aligned}
 \text{Moment about A,} \quad P_1 \times L_1 &= \frac{F_{\text{reb}}}{\sqrt{2}} \sum_{i=1}^n L_{\text{reb}}^i \\
 \text{Moment about B,} \quad P_2 \times L_2 &= \frac{F_{\text{reb}}}{\sqrt{2}} \sum_{i=1}^n L_{\text{reb}}^i \\
 F_R &= P_1 + P_2
 \end{aligned}
 \tag{1}$$

where L_1, L_2 is the distance of reaction force from the point of rotation, n is the number of reinforcing bars, F_{reb} is the reinforcing bar tensile strength assuming fracture stress of 650 MPa, and L_{reb}^i is the distance of i th reinforcing bar from the point of rotation in the free body. Using Eq. (1), the value of predicted resisting force F_R for fracture of reinforcing bar is 33.27 kN which closely represents the resisting force observed for the ER-RM specimen in Fig. 13.

Bond slip failure mechanism

Bond slip failure was seen for all the PCP bonded specimens with slip zones illustrated in Fig. 15 for Mode-1, Mode-2 and Mode-3 failure modes respectively. For failure Mode-1, there were three slip zones, failure Mode-2 and Mode-3 had two and three slip zones respectively. The bond slip zones have been identified considering the available slip lengths, where critical slip zones involve the ones having the least slip lengths. For equilibrium of forces of free bodies in Fig. 15, the approximate resisting force can be computed with proper assumption of the bond strength of each of the PCP used. The expression for equilibrium of forces can be

$$P_1 \times L_1 = \frac{\tau_b^{\text{avg}}(L_c)}{\sqrt{2}} \sum_{j=1}^m (L_{\text{slip}}^j \times L_j)$$

$$P_2 \times L_2 = \frac{\tau_b^{\text{avg}}(L_c)}{\sqrt{2}} \sum_{j=1}^m (L_{\text{slip}}^j \times L_j) \quad (2)$$

$$F_R = P = P_1 + P_2$$

where τ_b^{avg} is the average bond strength for the bonding agent, m is the number of slip zones, L_{slip}^j is the slip length of the j th slip zone, L_c is the circumferential length of the bond slip zone, and L_j is the distance of j th slip zone from the point of rotation in the free body. Taking an average value of τ_b^{avg} equal to 5 MPa, the least value of predicted resisting force, F_R , among three failure mechanisms is computed to be 23 kN from Eq. (2). The theoretically computed resisting force is plotted and compared against the experimentally observed ones in Fig. 13.

4. Finite element modeling

4.1 Model generation

The out-of-plane response of URM walls is highly nonlinear and is often governed primarily by cracking at mortar joints and rocking resistance due to gravity, rather than compressive failure of masonry and mortar materials. Masonry walls can be represented, with entire mortar joint by interface element (Lourenco and Rots 1997). With this approach, the failure of brick-mortar interface is not distinguished from that of mortar layer itself. In this paper, complete two dimensional (2D) FE models were generated and analyzed using the general purpose FE program DIANA9.3 (2008). Masonry walls were modeled by assuming that brick units are fully elastic and material nonlinearity was concentrated on truss elements and interface elements. Rocking resistance due to gravity is incorporated by considering geometrical nonlinearity.

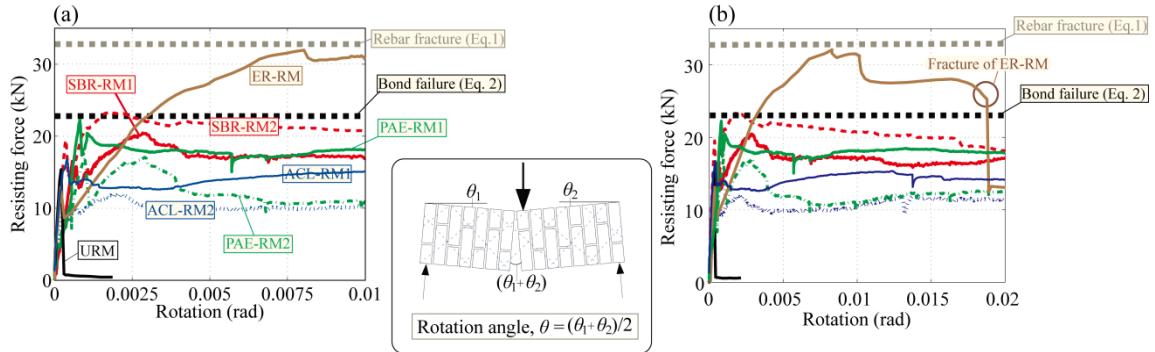


Fig. 13 Bending test results for all specimens: (a) Rotation angle < 0.01 radian, (b) Rotation angle > 0.01 rad

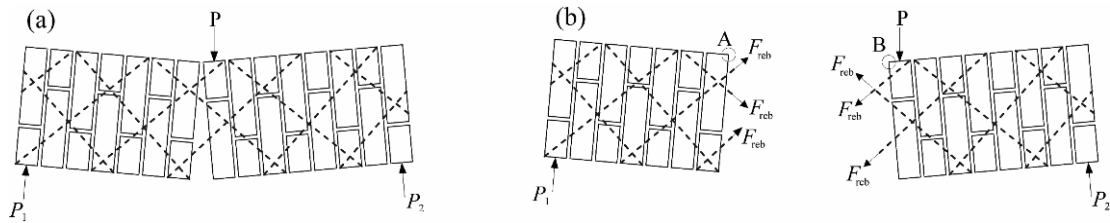


Fig. 14 Failure mode for ER-RM with fracture of reinforcing bar: (a) Deformed shape, (b) Free body diagram

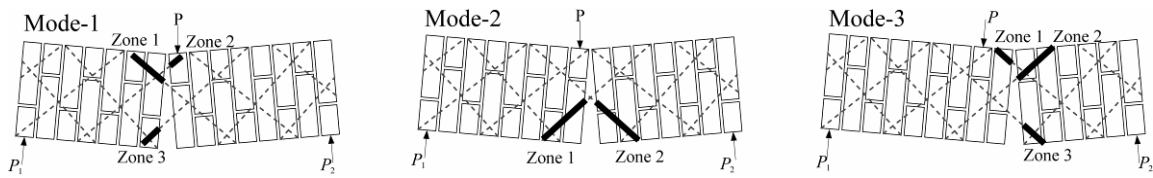


Fig. 15 Bond slip zones for failure Mode-1 (SBR-RM1 and SBR-RM2), Mode-2 (URM and ACL-RM1), Mode-3 (ACL-RM2, PAE-RM1 and PAE-RM2)

Special bond slip interface element shown in Fig. 16 was incorporated in the FE model. It should be noted that bond slip interface was modeled only for the pins inserted near the center of the specimen, where majority of cracks, reinforcement yielding and bond slips were observed during the experimentation. Another notable assumption was exclusion of horizontal mortar joint; only vertical mortar joints were modeled, since cracks were only observed in vertical mortar joints during tests. Main reasons for above assumption and confining of bond slip interfaces to certain zones were to reduce the model complexity and to get better solution convergence. Reinforcing bar truss elements with proper constitutive relations were used. The details of the elements used are described below.

4.1.1 Brick

As mentioned above, bricks were modeled to work perfectly elastic during the whole loading history and modeled with 2D four-node quadrilateral continuum elements. Material properties

used included Young’s modulus $E_b = 12$ GPa, Poisson’s ratio $\nu_b = 0.15$, and density, $\rho_b = 2000$ kg/m³ taken for typical masonry bricks (Oliveira *et al.* 2006).

4.1.2 Interface

Entire mortar joint was represented by brick unit/mortar interface. The interface model used in this study is implemented in DIANA9.3 (2008) as linear interface elements between two lines (2+2 nodes). The constitutive model adopts a discrete crack initiation criterion of normal traction characterized by full reduction of strength after the strength criterion has been violated. A discrete crack arises if the normal traction exceeds the tensile strength of mortar, f_t , with linear elastic behavior in compression. The normal stiffness of $D_{11} = 82$ N/mm³ and the shear stiffness of $D_{22} = 36$ N/mm³ were adopted for the brick/mortar interface (Lourenco and Rots 1997). Here, the tensile strength of mortar is assumed to be $f_t = 1.0$ MPa; the value derived from the tensile adhesion tests of interface between the brick units. The value assumed is slightly higher than the one corresponding to cracking of mortar joint in URM specimen which comes to be around 0.7 MPa.

The bond slip model proposed by Dörr (DIANA9.3 2008) was used to represent the interface between reinforcing bars and bricks. The model uses a polynomial relation between shear traction and slip (Shrestha *et al.* 2011c; Shrestha *et al.* 2013) which shows a limit if the slip is larger than a certain value dt^0 as illustrated in Fig. 17. The formulation for shear traction t_t is given by a cubic function:

$$t_t = \begin{cases} \tau_b \left(2.6 \left(\frac{dt}{dt^0} \right) - 2.4 \left(\frac{dt}{dt^0} \right)^2 + 0.7 \left(\frac{dt}{dt^0} \right)^3 \right) & \text{if } 0 \leq dt < dt^0 \\ \tau_b & \text{if } dt \geq dt^0 \end{cases} \quad (3)$$

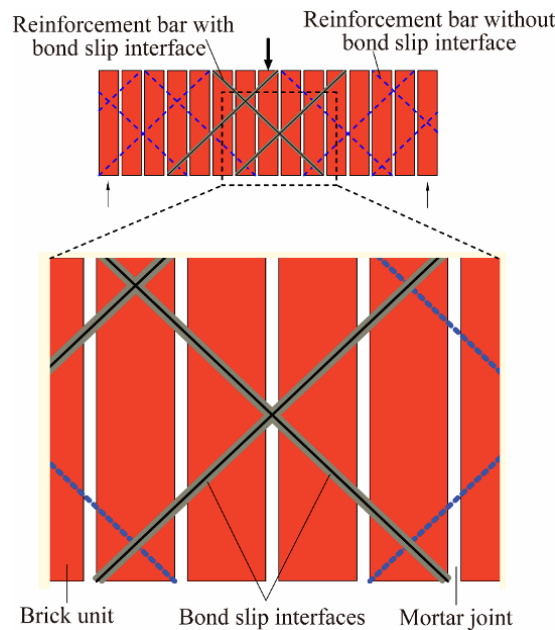


Fig. 16 FE model generation for bond-slip behavior of reinforcement bars

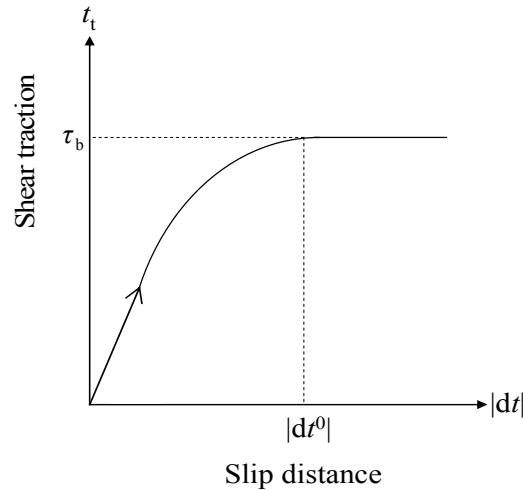


Fig. 17 Traction stress versus displacement plot for bond slip interface

where τ_b is the slip strength and $dt^0 = 0.06\text{mm}$ is the limiting slip distance. Based on the bond strength computation performed for experimental observation presented in Section 3.2, the value of τ_b in numerical model was varied from 1MPa up to 5MPa to account for the variability observed during the tests, for each PCP type.

4.1.3 Reinforcing bar

Steel reinforcements were represented by two-node truss elements with material properties representing steel bars given by elastic perfectly plastic properties adopting Young's Modulus for steel $E_{st} = 200\text{ GPa}$, yield stress $f_y = 650\text{ MPa}$ and diameter 5.5 mm.

4.2 Results

4.2.1 Sensitivity with variation in bond strength

Fig. 18(a) shows sensitivity results for FE models with slip strength τ_b equal to 1 MPa, 2 MPa, 3 MPa, 4 MPa and 5 MPa. Variation in bond strength directly influenced the resisting force characteristics, with larger bond slip strength corresponding to higher resistance and vice versa. Also for all models, almost constant restoring force was observed after initiation of slip at the bond slip interfaces. Similar failure mechanisms were observed for all the models, with slips at the bond slip interfaces as shown in Fig. 19. Here as a representative example, deformed shape for FE model with τ_b equal to 5 MPa has been presented, where dark regions highlighted by dotted markers represent the bond-slip zones. Since 5 MPa of average bond strength closely corresponds to the value observed for SBR PCPs, this particular FE model is represented as FE-RM^{SBR} from here onwards.

4.2.2 Comparison with experimental observations and theoretical predictions

The failure mechanism observed during experimentation showed mortar cracking and subsequent bond slips in three different modes as described in Section 3.3.2 and Fig. 15. The FE

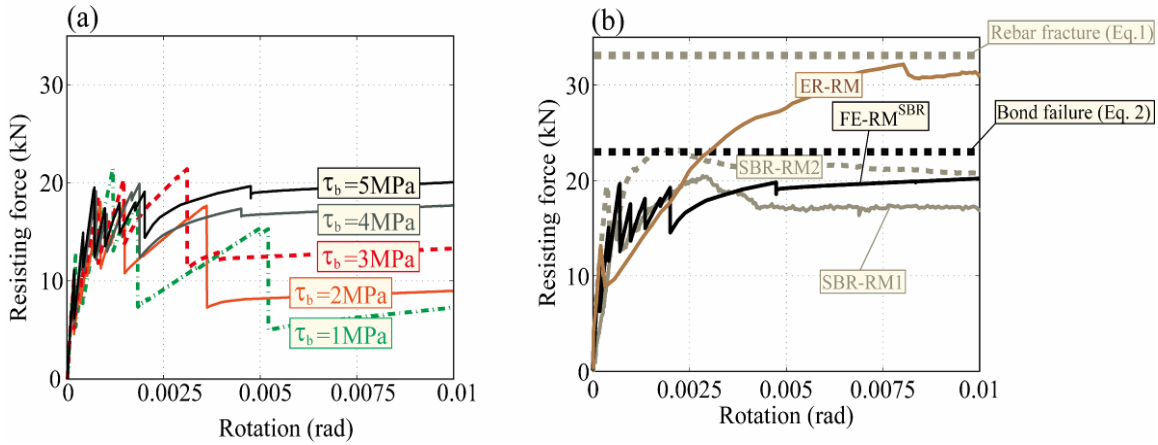


Fig. 18 Comparison on: (a) FE sensitivity study at varying bond strengths, (b) experimental and FE bending test results

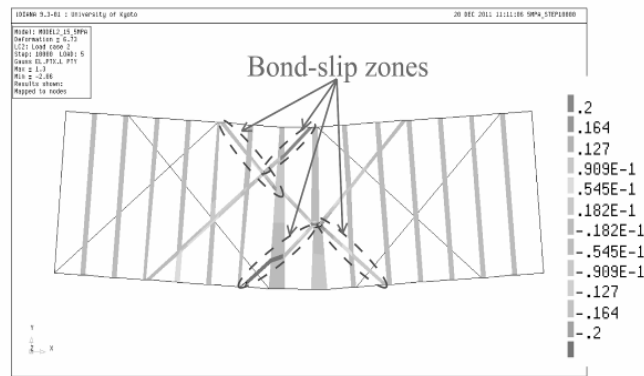


Fig. 19 FE deformed shape for τ_b equal to 5 MPa (FE-RM^{SBR})

model represented comparatively similar failure mode as shown in Fig. 19 just to the left and right mortar joint from the center of the specimen with slips at interfaces similar to the ones observed for experimental observations. Here, results have been plotted in Fig. 18(b), for FE-RM^{SBR} model with τ_b equal to 5 MPa, and compared correspondingly with SBR-RM specimens. FE result plotted against the experimental observations showed comparable response, with initial peak response corresponding to mortar tensile cracking and almost constant restoring force with initiation of slip at all critical bond slip zones. In both the cases, sharp decrement in resisting force measured was attributed to bond slip of interface element, followed by subsequent cracking of mortar joint interface. Furthermore, for the selected FE model, the post peak response, with residual resisting force after initiation of slip, closely predicted the theoretically computed post peak resistance for average bond strength τ_b^{avg} of 5 MPa.

5. Discussions

As shown in the previous sections, extensive experimental works were done to investigate

applicability of each type of PCP as bonding agent in masonry retrofitting. There were strong cases of increment in workability environment for the PCP bonded specimens, with open time set even at 10 minutes. However, pull-out tests and bending tests done on masonry assemblages showed contrasting results for each type of PCPs. It was found that there has to be proper and careful selection of PCP so as to achieve better resistance at superior workability environment. This section confers the above issue in detail.

5.1 PCP over epoxy bond

Epoxy resin, in its hardened state, has relatively higher stiffness with bond strength higher than strength of reinforcing bars used. The epoxy resin, when used as a bonding agent in masonry retrofitted specimens and loaded under superimposed load, has strong possibility of resulting in stress concentration at small section of reinforcing bar. This was seen during three-point bending experimentation for ER-RM beam specimen, where stress concentration resulted in brittle fracture of the steel bar at relatively smaller rotation angle of 0.018 radian as shown in Fig. 13(b). However, the response of PCP-RM specimens differed considerably. In case of PCP-RM specimens, relatively lower stiffness of PCP and bond strength lower than the strength of reinforcing bar resulted in stress distribution to large section of reinforcing bars. This in turn showed comparatively better ductile behavior for all the PCP-RM specimens; especially for SBR-RM specimens which showed better resistance to superimposed load without sudden fracture of reinforcing bars used. On these accounts, SBR PCP as bonding agent facilitates both cost effectiveness as well as performance enhancement over epoxy resin.

5.2 Choice of PCP based on its workability and bond strength

Series of workability and pull-out tests were performed on specimens with available combinations of PCPs and impregnants showing improvement in workability condition, even with open time set at 10 minutes. However, water treated specimens also showed good workability as illustrated in Fig. 10 for EVA, SBR1 and SBR2 injected specimens and better bond strength as shown in Fig. 12. Nevertheless, it should be noted that the experimental tests were performed in an idealistic condition with well-cut bricks, which is particularly different to that in actual practice, with old brick masonry and porous mortar joints. This possibly makes water treated specimens show contradictory behavior to the one observed in this study, when performed in real practice in highly porous media. Additionally, it is very difficult to pour water in to the drilled hole uniformly, due to its low viscosity, which possibly results in non-uniform distribution of dry and wet surfaces. Therefore, there may be large variability for water treated specimens in actual practice making their use less appealing. A better control of loss of water, and uniformity in pouring can be done with use of impregnants, whose viscosity can be effectively controlled. This would require the selection of proper water penetration barrier reagents prior to PCP injection which results in an improved workability without affecting the actual strength of PCP.

Fig. 20 shows the consistency of results from pull-out tests in terms of bond strength and its coefficient of variation at different open times for combinations of PCPs and impregnants. EVA, ACL and PAE specimens showed large variations in the test data with coefficients of variations for EVA up to 17%, ACL 38% and PAE 52% which shows strong uncertainty over the strength of these PCPs used in combination with impregnants. SBR1 and SBR2 specimens on the other hand showed relatively consistent bond strength data for the series of tests done. Hence, among the

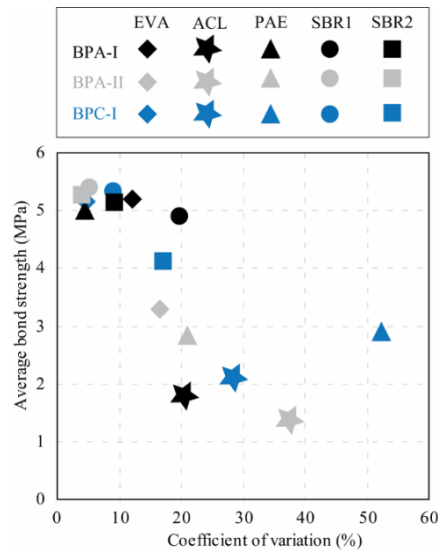


Fig. 20 Coefficient of variation of the pull-out test data on specimens

impregnants used, the best combination of PCP and pretreatment agent showing strong bond with minimum strength variation at different open times was attained for SBR PCPs with BPA-II as pretreatment agent.

6. Conclusions

Experimental works were done to compare the workability and bond strength of different polymer-cement pastes (PCPs) - EVA, ACL, PAE, SBR1 and SBR2, in brick masonry.

Additionally, three-point bending test was also performed to compare the effectiveness of particular PCPs in masonry assemblages followed by FE simulations of the experimental works. Based on these works, the following conclusions can be drawn:

- (1) Results of workability tests showed properly selected PCPs are highly workable, even at adverse working conditions with the open time of 10 minutes. The workability test also showed the importance of pre-treatment agents or impregnants, as water penetration barrier system, to increase the workability of PCP, effectively avoiding the loss of water from PCP. The untreated and polymer treated specimens showed poor performance whereas, either of impregnants BPA-I, BPA-II, BPC-I or water as pretreatment agents resulted in substantial increment of workability for EVA, PAE and SBR PCPs.
- (2) From the pull-out test results, ACL and PAE have least bond strength, as compared to EVA, SBR1 and SBR2 PCPs. Observed bond strengths of EVA, SBR1 and SBR2 PCPs were in the range of 5 MPa or more, which represents extremely superior bond strength.
- (3) Three-point bending tests performed showed ACL and PAE bonded RM specimens have relatively lower resistance, due to premature bond slip of the reinforcing bars. SBR PCP bonded RM specimen represented better resistance and ductility mainly due to better bond strength of SBR PCP. Epoxy bonded RM specimen showed comparatively higher resistance but with significantly lower ductility resulting in brittle failure.

- (4) Proposed theoretical and FE prediction also showed response comparable to the experimental observations. Sensitivity analysis performed for the FE models showed strong dependence of RM specimens' response over the bond strength of bonding agents used.
- (5) Series of workability tests, pull-out tests and three-point bending tests performed on pinning retrofitted masonry assemblages showed that combination of SBR PCP, with pretreatments by either impregnants or water, resulted in strong bond with minimum strength variation at different open times. However, it should be noted that the use of water as pretreatment agents would require more careful and proper monitoring in highly porous media especially found in historical masonry structures.

Acknowledgments

This work was supported by Grant-in-Aid for Scientific Research (B) No. 20360253 and by the Global COE Program, provided by the Japan Society for the Promotion of Science (JSPS). Part of this research was also supported by Obayashi Foundation. The authors would also like to acknowledge the technical assistance of Mr. Shinnousuke Kaneuchi and Mr. Hiroki Sekine of Nihon University in undertaking the experimental works. The authors would also like to acknowledge the anonymous reviewers for their comments and questions, which led to significant improvement of the manuscript.

References

- Abrams, D., Smith, T., Lynch, J. and Franklin, S. (2007), "Effectiveness of rehabilitation on seismic behavior of masonry piers", *J. Struct. Eng. - ASCE*, **133**(1), 32-43.
- Anagnostopoulos, C.A. and Anagnostopoulos, A.C. (2002), "Polymer-cement mortars for repairing ancient masonries mechanical properties", *Constr. Build. Mater.*, **16**(7), 379-384.
- Ashraf, M., Khan, A.N., Naseer, A., Ali, Q. and Alam, B. (2012), "Seismic behavior of unreinforced and confined brick masonry walls before and after ferrocement overlay retrofitting", *Int. J. Archit. Heritage*, **6**(6), 665-688.
- Calderini, C. (2008), "Use of reinforced concrete in preservation of historic buildings: conceptions and misconceptions in the early 20th century", *Int. J. Archit. Heritage*, **2**(1), 25-59.
- Curti, E., Podesta, S. and Resemini, S. (2008), "The post-earthquake reconstruction process of monumental masonry buildings: Suggestions from the Molise event (Italy)", *Int. J. Archit. Heritage*, **2**(2), 120-154.
- DIANA (2008), *DIANA User's Manual Release 9.*, TNO DIANA BV, Delft, Netherlands.
- Faella, C., Martinelli, E., Nigro, E. and Paciello, S. (2010), "Shear capacity of masonry walls externally strengthened by a cement-based composite material: An experimental campaign", *Constr. Build. Mater.*, **24**(1), 84-93.
- Fowler, D.W. (1999), "Polymers in concrete: a vision for the 21st century", *Cement Concrete Comp.*, **21**(5-6), 449-452.
- Kikuchi, K., Kuroki, K., Toyodome, M., Escobar, C. and Nakano, Y. (2008), "Seismic retrofit of unreinforced clay brick masonry wall using polymer-cement mortar", *Proceedings of 14th World Conference on Earthquake Engineering*, Beijing, China, October.
- Lourenco, P.B. and Rots, J.G. (1997), "Multisurface interface model for analysis of masonry structures", *J. Eng. Mech.*, **123**(7), 660-668.
- Maranhao, F.L. and John, V.M. (2009), "Bond strength and transversal deformation aging on cement-polymer adhesive mortar", *Constr. Build. Mater.*, **23**(2), 1022-1027.

- Ohama, Y. (1995), *Handbook of polymer-modified concrete and mortar, properties and process technology*, Noyes Publications, New Jersey, USA.
- Ohama, Y. (1998), "Polymer-based admixtures", *Cement Concrete Comp.*, **20**(2-3), 189-212.
- Oliveira, D.V., Lourenco, P.B. and Roca, P. (2006), "Cyclic behaviour of stone and brick masonry under uniaxial compressive loading", *Mater. Struct.*, **39**(286), 247-257.
- Pareek, S. and Kuroda, K. (2003), "Evaluation of polymer-cement pastes as bonding agents for flexural strengthening of RC beams by continuous fiber sheets", *Proceedings of Intern. Symposium on Latest Achievement of Techno. Rese. Retrofitting Concrete Struct.*, Kyoto, Japan.
- Shrestha, K.C., Nagae, T. and Araki, Y. (2011a), "Finite element modeling of cyclic out-of-plane response of masonry walls retrofitted by inserting inclined stainless steel bars", *J. Disaster Res.*, **6**(1), 36-43.
- Shrestha, K.C., Nagae, T. and Araki, Y. (2011b), "Finite element study on pinning retrofitting technique of masonry walls with opening subjected to in-plane shear load", *ACEE-J.*, **4**(4), 81-96.
- Shrestha, K.C., Araki, Y., Nagae, T., Omori, T., Sutou, Y., Kainuma, R. and Ishida, K. (2011c), "Applicability of Cu-Al-Mn shape memory alloy bars to retrofitting of historical masonry constructions", *Earthq. Struct.*, **2**(3), 233-256.
- Shrestha, K.C., Araki, Y., Nagae, T., Omori, T., Sutou, Y., Kainuma, R. and Ishida, K. (2013), "Effectiveness of superelastic bars for seismic rehabilitation of clay-unit masonry walls", *Earthq. Eng. Struct. Dyn.*, **42**(5), 725-741.
- Takiyama, N., Nagae, T., Maeda, H., Kitamura, M., Yoshida, N. and Araki, Y. (2008), "Cyclic out-of-plane flexural behavior of masonry walls rehabilitated by inserting steel pins", *Proceedings of 14th World Conference on Earthq. Eng.*, Beijing, China, October.
- Willis, C.R., Seracino, R. and Griffith, M.C. (2010), "Out-of-plane strength of brick masonry retrofitted with horizontal NSM CFRP strips", *Eng. Struct.*, **32**(2), 547-555.